arXiv:0806.1414v1 [physics.atom-ph] 9 Jun 2008

Absolute frequency measurement of the $^{40}Ca^+$ $4s\ ^2S_{1/2} - 3d\ ^2D_{5/2}$ clock transition

M. Chwalla,[1] J. Benhelm,[1,2] K. Kim,[1,*] G. Kirchmair,[1,2] T. Monz,[1] M. Riebe,[1] P. Schindler,[1] A. S. Villar,[1] W. Hänsel,[1] C. F. Roos,[1,2,†] R. Blatt,[1,2] M. Abgrall,[3] G. Santarelli,[3] G. D. Rovera,[3] and Ph. Laurent[3]

[1] *Institut für Experimentalphysik, Universität Innsbruck, Technikerstrasse 25, A–6020 Innsbruck, Austria*
[2] *Institut für Quantenoptik und Quanteninformation der Österreichischen Akademie der Wissenschaften, Technikerstrasse 21a, A–6020 Innsbruck, Austria*
[3] *LNE-SYRTE, Observatoire de Paris, 61, Avenue de l'Observatoire, 75014 Paris, France*

(Dated: June 9, 2008)

We report on the first absolute transition frequency measurement at the 10^{-15} level with a single, laser-cooled $^{40}Ca^+$ ion in a linear Paul trap. For this measurement, a frequency comb is referenced to the transportable Cs atomic fountain clock of LNE-SYRTE and is used to measure the $^{40}Ca^+$ $4s\ ^2S_{1/2}$–$3d\ ^2D_{5/2}$ electric-quadrupole transition frequency. After the correction of systematic shifts, the clock transition frequency $\nu_{Ca^+} = 411\,042\,129\,776\,393.2(1.0)$ Hz is obtained, which corresponds to a fractional uncertainty within a factor of three of the Cs standard. Future improvements are expected to lead to an uncertainty surpassing the best Cs fountain clocks. In addition, we determine the Landé g-factor of the $3d\ ^2D_{5/2}$ level to be $g_{5/2}$=1.2003340(3).

PACS numbers: 32.30.Jc,06.30.Ft,37.10.Ty,32.80.Qk

Fostered by the advent of the optical frequency comb technology, there is currently a strong trend towards the development of optical frequency standards that are expected to replace the current microwave standard in cesium as the basis of the definition of the SI second. Recently, the best optical frequency standards, based on single trapped ions and neutral atoms held in optical lattices respectively [1, 2], have both demonstrated a fractional frequency uncertainty of 10^{-16} or even better, thus surpassing the best cesium fountain clocks. The great attraction of optical frequency standards lies in the superior resonance line quality factors, allowing shorter averaging times and higher stability. Experiments with single, trapped ions have provided key contributions to the field of optical clocks and precision measurements in the past 20 years [3]. Several candidates for an optical ion clock have been investigated such as Hg^+, Al^+, Yb^+, In^+, Sr^+ [4, 5, 6, 7, 8, 9], or proposed like Ca^+ [10, 11].

Building an ion clock based on Ca^+ has the technological advantage that all necessary wavelengths for laser cooling and state manipulation including lasers for photoionization can be generated by commercially available and easy-to-handle solid state lasers. Fig. 1 shows the relevant atomic levels of the isotope $^{40}Ca^+$. The actual clock transition considered here is the electric quadrupole transition from the $4s\ ^2S_{1/2}$ to the $3d\ ^2D_{5/2}$ level, which has a natural lifetime of 1.17 s [12]. A non-zero magnetic field lifts the Zeeman degeneracy and splits the transition into ten lines. Probing several of them provides a means to cancel the most important systematic effects like the linear Zeeman and the electric quadrupole shift [9].

An overview of our experimental setup is given in Fig. 2. We use a linear Paul trap [14] with four blades separated by 2 mm and two tips of 5 mm separation providing radial and axial confinement. Applying a radio-frequency (RF) power of 9 W to the trap and setting

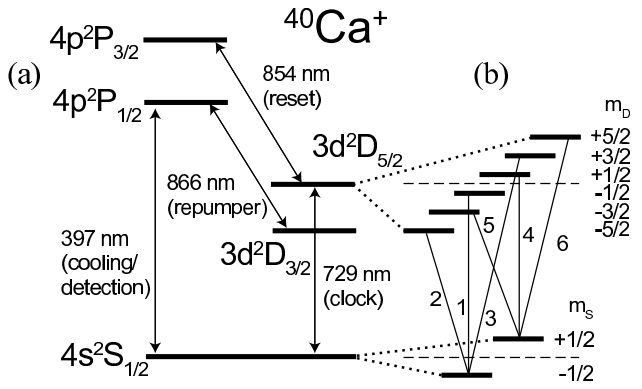

FIG. 1: (a) Partial level scheme of $^{40}Ca^+$ showing the $S_{1/2} - D_{5/2}$ clock transition as well as the transitions used for resetting, repumping, cooling, and detecting the ion. (b) Magnetic sub-levels of the clock transition and the six transitions having the biggest coupling strength for the actual laser polarization, quantization axis, and k-vector of the laser at 729 nm. The numbers indicate the order in which the transitions were probed.

the tips to a potential of 1000 V, we achieve typical secular trap frequencies $\omega_r/2\pi$=3.9 MHz in the radial and $\omega_a/2\pi$=1.2 MHz in the axial direction. Single Ca^+ ions are loaded into the trap by photo-ionizing a beam of neutral calcium atoms.

A frequency measurement cycle consisted of 2 ms of Doppler cooling on the $S_{1/2} - P_{1/2}$ at a wavelength of 397 nm and repumping at 866 nm and 854 nm to prevent pumping into the $D_{3/2}$ level and to clear out population from the $D_{5/2}$ level. State initialization was achieved by optical pumping into $|S_{1/2}, m_S = -1/2\rangle$. After that, laser pulses at 729 nm from a titanium-sapphire laser, which was locked to a high finesse cavity similar in design to the one described in ref. [17], were used to probe the

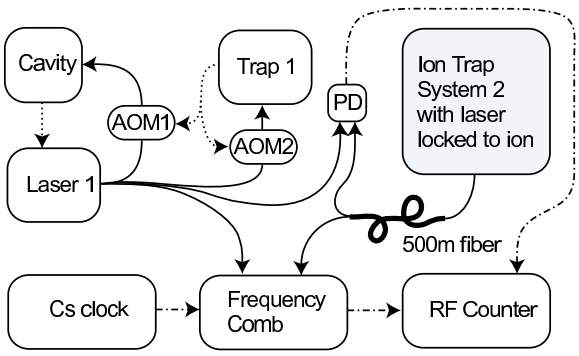

FIG. 2: Experiment setup: The frequency of an ultra-stable laser is locked to a single $^{40}Ca^{+}$ stored in a linear ion trap and measured by a frequency comb referenced to a transportable Cs fountain atomic clock. The light of a second laser locked in a similar manner to another trap system in another lab is transported via a 500 m long optical fiber link. An optical beat note is detected on a fast photodiode (PD). The solid lines are optical signals, the dotted lines indicate electronic feedback and the dashed-dotted lines show RF signals.

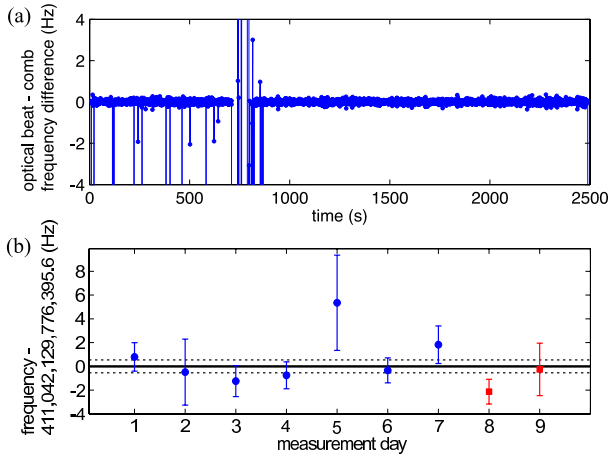

FIG. 3: (a) Example for a data set where the direct optical beat signal of both lasers was compared to the difference of the frequency comb readings. This information was used to detect cycle slips of the counters (gate time 1 s) mainly caused by low signal-to-noise ratio. An error shows up as a frequency difference larger than 1 Hz. (b) Frequency deviation during different days. The circles are mean values with statistical error bars (1σ) for normal trap drive power of 9 W. The solid line is the average of this data with the statistical uncertainty indicated by dashed lines. The squares show data obtained with the trap power reduced by a factor of three.

$S_{1/2} - D_{5/2}$ transition. From an optical beat note with a similar laser system we infer a typical linewidth (FWHM) of 50 Hz over 40 minutes. A constant magnetic field of 3.087(2) G splits the Zeeman multiplet into ten components, six of which (Δm=0 or $|\Delta m|$=2) could be excited with good coupling strength in the geometry chosen for the laser polarization, k-vector, and magnetic field [15]. To probe transitions starting from $|S_{1/2}, m_S = +1/2\rangle$, the level was populated by two π-pulses transferring the population from $|S_{1/2}, m_S = -1/2\rangle$ via the state $|D_{5/2}, m_D = +1/2\rangle$. The transition frequencies were probed by Ramsey experiments with the pulse lengths of the $\pi/2$ pulses adjusted to $\tau = 50\,\mu$s. A Ramsey probe time of $T_R = 1$ ms yielded a minimum contrast of 86% on the transition most sensitive to magnetic field fluctuations. After the Ramsey excitation, the state of the ion was detected by electron shelving using a photo multiplier for fluorescence detection. A detection time of 2 ms led to a state discrimination efficiency well above 99%. This cycle was repeated a hundred times to obtain the mean excitation probability. To infer the line center of a transition, we switched the relative phase of the Ramsey pulses by 90° with a precision of better than $\pi \times 10^{-4}$ and repeated the experiment with reversed pulse order. This arrangement is free of errors due to incorrectly set phases.

The dominant level shifts caused by electro-magnetic fields are the linear Zeeman shift ($\propto 10$ MHz) induced by the static magnetic field defining the quantization axis and the electric quadrupole shift ($\propto 10$ Hz), resulting from an interaction of the quadrupole moment of the $3d\,^2D_{5/2}$ level [13] with static electric field gradients caused by either the DC-trapping fields and possible spurious field gradients of patch potentials. Both level shifts cancel out when averaging over all frequency measurements of the six transitions shown in Fig. 1(b).

The six transitions were repeatedly probed in the order shown in Fig. 1(b) in a measurement cycle taking 22 s, and the mean excitation and the frequencies of all acousto-optical modulators (AOM) for each setting were recorded. The measurement results obtained from transitions 1 and 4 ($|m_S = -1/2\rangle \leftrightarrow |m_D = -1/2\rangle$ and $|m_S = +1/2\rangle \leftrightarrow |m_D = +1/2\rangle$) were used to infer the current laser frequency relative to the ion and the magnetic field strength. This information was fed back onto the frequency of acousto-optic modulators (see Fig. 2) to compensate for slow drifts of the reference cavity (AOM1) and the magnetic field (AOM2). Together with a measurement of the quadrupole shift as described in [16], we were able to predict the individual transition frequencies within the statistical measurement accuracy of ± 0.4 Hz which is within a factor of two of the expected quantum projection noise. The individual transition frequency data combined with the Landé g-factor of the $S_{1/2}$ level [19] was used to determine the g-factor of the $D_{5/2}$ level to be g_D=1.2003340(3).

A part of the probe laser light was sent to a frequency comb for a measurement of its frequency. The frequency comb as well as all radio frequency sources in the experiment, i. e. synthesizers for AOMs tuning the laser into resonance with the ion or cancelling fiber noise, were referenced to the transportable Cs fountain atomic clock of LNE-SYRTE which has an accuracy of better than 10^{-15} [18] as was also confirmed by comparison of the fountain clock with the ensemble of fountains in Paris

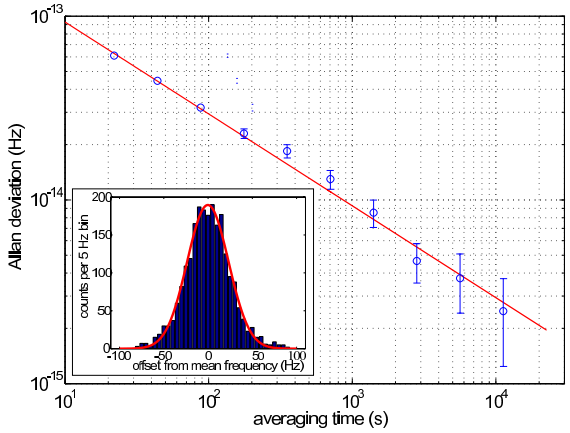

FIG. 4: Absolute frequency instability for the comparison of $^{40}Ca^{+}$ against Cs. The data set consists of 2278 frequency measurement sets of all six transitions with an effective gate time of 22 s. The inset shows a histogram of the data which is consistent with a Gaussian fit of 23(1) Hz standard deviation.

before and after the experiment. The second ion trap experiment (see Fig. 2) served to check the validity of the frequency comb readings. Three synchronized counters with a respective gate time of 1 s counted the beat note frequency f_B of the two lasers, the beat note frequency f_1 of the comb with the first laser and the beat note frequency f_2 of the comb with the second laser. If $||f_1 - f_2| - f_B| \geq 0.5\,\mathrm{Hz}$, the measurement was removed (see Fig. 3(a)). The recorded measurement data was combined in the following way: the AOM frequencies applied for each transition and the respective frequency deviations inferred by the Ramsey experiments were averaged together with the frequency comb data in the same time window. The computers for data taking were synchronized to better than 0.1 s. The frequency of the $4s\ ^2S_{1/2} - 3d\ ^2D_{5/2}$ transition without correction for systematic shifts could be determined to be 411 042 129 776 395.6(0.5) Hz, limited mainly by the stability of the frequency comb's repetition rate. The average frequency per day is given in Fig. 3(b). The Allan standard deviation for the data is shown in Fig. 4. The solid line is a fit with $\sigma_y(\tau) = 2.9(1) \times 10^{-13}\ \tau^{-1/2}$, suggesting white frequency noise as the dominant noise source. The inset shows a histogram of the deviation from the average frequency which fits a Gaussian distribution with 23(1) Hz standard deviation.

The influence of the most important effects on the transition frequency with their magnitude and uncertainty is given in Tab. I. Since the linear Zeeman shift, the electric quadrupole shift as well as the AC-Zeeman shift caused by imbalanced currents in the trap electrodes cancel by the chosen measurement scheme, the largest remaining shift is due to the second order Zeeman effect which we determined to be 1.368(1) Hz at a mean magnetic field of 3.087(2) G. There was also a residual magnetic field drift which on average was $2(1)\cdot10^{-8}$ G/s. This lead to a measurement offset of 28(14) mHz because this effect is not completely canceled by averaging over the six transitions without changing their order.

However, the largest uncertainty in the error budget stems from the AC-Stark shift induced by black body radiation. The ion is exposed to thermal fields emanating from the surrounding vacuum vessel and the ion trap which gets heated up by the applied RF power. These shifts can be calculated given the static scalar polarizabilities of the $S_{1/2}$ and $D_{5/2}$ states [20]. The actual trap temperature as a function of the applied RF power can only be roughly estimated with the help of a test setup similar to the ion trap we were using for the frequency measurement. At the input power of 9 W that was applied for the frequency measurement, the trap heats up to about 150±50 °C. The trap only covers about one third of the total solid angle while the rest is covered by the surrounding vacuum vessel at a temperature of 25±2 °C, we estimate the black body shift to be 0.9(7) Hz. The last two data points of Fig. 3(b) show measurements taken at a lower trap power (3 W) and therefore lower trap temperature (60±20 °C). At this level, no difference is apparent as the expected frequency difference due to the change in black body radiation is on the order of -0.4(4) Hz.

The Ramsey experiment leads to an AC-Stark shift $\delta_{probe} = \delta_{AC}/(\frac{\pi T_R}{4\tau} + 1)$, where T_R is the probe time and δ_{AC} the light shift during the time τ of the Ramsey pulses which is mostly caused by non-resonant excitation of dipole transitions [15]. For our parameters, the expected shift is 0.11(2) Hz. The light shift induced by the residual light of the resetting laser at 854 nm could be measured to be -0.005(4) Hz. The shifts by the cooling laser at 397 nm and the repumping laser at 866 nm are estimated by a worst case scenario: the residual amount of light which could be detected is assumed to be focused tightly onto the ion. For the cooling laser we assume a detuning of half a linewidth where the shift would be maximum. The corresponding shifts and the uncertainties are well below 0.1 Hz. Excess micromotion induced by the trapping field [21] is responsible for second order Doppler and AC-Stark shifts. With the help of additional DC electrodes, we compensate micromotion to modulation indices smaller than 1%, resulting in micromotion-related frequency errors of 0.1 Hz at most. Taking into account these systematic shifts, the corrected value of the $4s\ ^2S_{1/2} - 3d\ ^2D_{5/2}$ transition is $\nu_{Ca^+} = 411\,042\,129\,776\,393.2(1.0)$ Hz which corresponds to $2.4 \cdot 10^{-15}$ relative uncertainty. To our knowledge, this is the most accurate of any Ca^+ transition frequency measurement so far [22].

It appears realistic that an experiment with $^{40}Ca^{+}$ especially designed for metrology could lead to an accuracy of better than 10^{-16}–10^{-17}. There are some advances necessary to reach this level such as improved light attenuation when switching off the lasers in order to eliminate

TABLE I: The systematic frequency shifts and their associated errors in Hz and the fractional uncertainty in units of 10^{-15}.

Effect	**Shift (Hz)**	**Error (Hz)**	**Fractional err.** (10^{-15})
Statistical error	-	0.5	1.2
1^{st}-order Zeeman	0	0.2	0.5
Magnetic field drift	0.03	0.01	0.02
2^{nd}-order Zeeman: quantization field	1.368	0.002	0.005
Electric quadrupole	0	0.2	0.5
AC Stark shifts:			
Laser at 729 nm	0.11	0.04	0.1
Lasers at 397, 866, and 854 nm	0	< 0.1	< 0.2
Black body rad.	0.9	0.7	1.7
Micromotion	0	0.1	0.2
2^{nd}-order Doppler	-0.001	0.001	0.002
Cs uncertainty	0	0.4	1
Total shift	**2.4**	**1.0**	**2.4**

AC Stark shifts. It is more difficult to improve on the shift by black body radiation. For this, a new trap would have to be designed with the possibility to measure the trap temperature exactly. Additionally, operating the trap in a cryogenic environment [4] would dramatically reduce the frequency uncertainty due to the black body shift. Generally, a laser with enhanced stability could substantially improve on the required measurement time for investigating systematic effects by comparison of the two ion trap experiments.

Our experimental setup is mainly dedicated to processing quantum information, a field of research closely related to metrology: a pair of entangled ions can be used for improving the signal-to-noise ratio [23, 24] but also for designing states which are immune to certain kinds of environmental perturbations [13, 16]. States like $|S_{1/2}, m_S\rangle|S_{1/2}, -m_S\rangle + |D_{5/2}, m_D\rangle|D_{5/2}, -m_D\rangle$ which are immune against magnetic field fluctuations to first order could be used for generalized Ramsey experiments with probe times limited only by the probe laser stability and spontaneous decay of the metastable state. Preliminary tests with such states showed significant phase errors caused by changes in the optical path length in the electro-optical deflector used for steering the beam to enable individual addressing of the ions. To overcome this problem, beam steering of a strongly focused laser could be avoided by generating high-fidelity entanglement [25] with a laser beam collectively interacting with the ions, and combining this wide beam with a second strongly focused laser beam inducing phase shifts to make the ions distinguishable for carrying out coherent operations on a single ion.

This work was supported by the Austrian "Fonds zur Förderung der wissenschaftlichen Forschung", the Austrian Academy of Sciences, IARPA, the European network SCALA, and the Institut für Quanteninformation GmbH. The mobile fountain work is supported by CNES, CNRS, LNE and région Ile de France (IFRAF). The SYRTE is a unit associated to CNRS UMR 8630. We thank P. O. Schmidt and H. Häffner for fruitful discussions and a critical reading of the manuscript.

* Present adress: Department of Physics, University of Maryland, College Park, Maryland, 20742, USA
† christian.roos@uibk.ac.at

[1] A. D. Ludlow *et al.*, Science **319**, 1805 (2008).
[2] T. Rosenband *et al.*, Science **319**, 1808 (2008).
[3] A. A. Madej and J. E. Bernard, in *Frequency Measurement and Control* (ed. A. N. Luiten) pp.153–195 (Topics in Applied Physics Vol. 79, Springer Verlag, Berlin, 2001).
[4] W. H. Oskay *et al.*, Phys. Rev. Lett. **97**, 020801 (2006).
[5] T. Rosenband *et al.*, Phys. Rev. Lett. **98**, 220801 (2007).
[6] J. Stenger *et al.*, Opt Lett. **26**, 1589 (2001).
[7] P. J. Blythe *et al.*, Phys. Rev. A **67**, 020501(R) (2003).
[8] J. von Zanthier *et al.*, Opt. Lett. **25**, 1729 (2000).
[9] H. S. Margolis *et al.*, Science **306**, 1355 (2004).
[10] C. Champenois *et al.*, Phys. Lett. A **331**, 298 (2004).
[11] M. Kajita, Y. Li, K. Matsubara, K. Hayasaka, and M. Hosokawa, Phys. Rev. A **72**, 043404 (2005).
[12] P. Barton *et al.*, Phys. Rev. A **62**, 032503 (2000).
[13] C. F. Roos, M. Chwalla, K. Kim, M. Riebe, and R. Blatt, Nature **443**, 316 (2006).
[14] F. Schmidt-Kaler *et al.*, Appl. Phys. B **77**, 789 (2003).
[15] H. Häffner *et al.*, Phys. Rev. Lett. **90**, 143602 (2003).
[16] M. Chwalla *et al.*, Appl. Phys. B **89**, 483 (2007).
[17] M. Notcutt, L.-S. Ma, J. Ye, and J. L. Hall, Opt. Lett. **30**, 1815 (2005).
[18] S. Bize *et al.*, J. Phys. B **38**, S449 (2005).
[19] G. Tommaseo *et al.*, Eur. Phys. J. D **25**, 113 (2003).
[20] B. Arora, M. S. Safronova, and C. W. Clark, Phys. Rev. A **76**, 064501 (2007).
[21] D. J. Berkeland, J. D. Miller, J. C. Bergquist, W. M. Itano, and D. J. Wineland, J. Appl. Phys. **83**, 5025 (1998).
[22] Very recently, the transition frequency was also measured at NICT, Tokyo, yielding 411 042 129 776 385 ± 18 Hz, the value being consistent with our result. Private communication by Ying Li.
[23] J. J. Bollinger, W. M. Itano, D. J. Wineland, and D. J. Heinzen, Phys. Rev. A **54**, R4649 (1996).
[24] D. Leibfried *et al.*, Science **304**, 1476 (2004).
[25] J. Benhelm, G. Kirchmair, C. F. Roos, and R. Blatt, Nat. Phys. **4**, 463 (2008).